Published online 1 June 2016

Nucleic Acids Research, 2016, Vol. 44, No. 13 ***6335–6349***
doi: 10.1093/nar/gkw508

RNA topoisomerase is prevalent in all domains of life and associates with polyribosomes in animals

Muzammil Ahmad[1], Yutong Xue[1], Seung Kyu Lee[1], Jennifer L. Martindale[2], Weiping Shen[1], Wen Li[3], Sige Zou[4], Maria Ciaramella[5], Hélène Debat[6], Marc Nadal[6], Fenfei Leng[7], Hongliang Zhang[8], Quan Wang[9], Grace Ee-Lu Siaw[10], Hengyao Niu[9], Yves Pommier[8], Myriam Gorospe[2], Tao-Shih Hsieh[10,11], Yuk-Ching Tse-Dinh[7], Dongyi Xu[3,*] and Weidong Wang[1,*]

[1]Genome Instability and Chromatin Remodeling Section, Lab of Genetics, National Institute on Aging, National Institutes of Health, 251 Bayview Boulevard, Baltimore, MD 21224, USA, [2]RNA Regulation Section, Lab of Genetics, National Institute on Aging, National Institutes of Health, 251 Bayview Boulevard, Baltimore, MD 21224, USA, [3]State Key Laboratory of Protein and Plant Gene Research, School of Life Sciences, PeKing University, Beijing 1000871, China, [4]Translational Gerontology Branch, National Institute on Aging, National Institute of Health, 251 Bayview Boulevard, Baltimore, MD 21224, USA, [5]Institute of Biosciences and Bioresources, National Research Council of Italy, Naples 80131, Italy, [6]Institut Jacques Monod, CNRS-Université Paris Diderot-UMR7592, 15 rue Hélène Brion, 75205 Paris Cedex, France, [7]Department of Chemistry & Biochemistry, Biomolecular Sciences Institute, Florida International University, Miami, FL 33199, USA, [8]Developmental Therapeutics Branch and Laboratory of Molecular Pharmacology, Center for Cancer Research, National Cancer Institute, NIH, Bethesda, MD 20892, USA, [9]Molecular and Cellular Biochemistry Department, Indiana University, 212 South Hawthorne Drive, Bloomington, IN 47405, USA, [10]Institute of Cellular Organistic Biology, Academia Sinica, Taipei 11529, Taiwan and [11]Department of Biochemistry, Duke University Medical Center, Durham, NC 73532, USA

Received March 18, 2016; Revised May 06, 2016; Accepted May 25, 2016

ABSTRACT

DNA Topoisomerases are essential to resolve topological problems during DNA metabolism in all species. However, the prevalence and function of RNA topoisomerases remain uncertain. Here, we show that RNA topoisomerase activity is prevalent in Type IA topoisomerases from bacteria, archaea, and eukarya. Moreover, this activity always requires the conserved Type IA core domains and the same catalytic residue used in DNA topoisomerase reaction; however, it does not absolutely require the non-conserved carboxyl-terminal domain (CTD), which is necessary for relaxation reactions of supercoiled DNA. The RNA topoisomerase activity of human Top3β differs from that of *Escherichia coli* topoisomerase I in that the former but not the latter requires the CTD, indicating that topoisomerases have developed distinct mechanisms during evolution to catalyze RNA topoisomerase reactions. Notably, Top3β proteins from several animals associate with polyribosomes, which are units of mRNA translation, whereas the Top3 homologs from *E. coli* and yeast lack the association. The Top3β-polyribosome association requires TDRD3, which directly interacts with Top3β and is present in animals but not bacteria or yeast. We propose that RNA topoisomerases arose in the early RNA world, and that they are retained through all domains of DNA-based life, where they mediate mRNA translation as part of polyribosomes in animals.

INTRODUCTION

The first topoisomerase was discovered in *Escherichia coli* in 1971 (1). Since then, topoisomerases have been identified and characterized in numerous species from all domains of life. These enzymes are 'magicians of the DNA world', solving critical topological problems generated during DNA dynamics (2). Topoisomerases uniquely catalyze DNA strand passage reactions. Type I topoisomerases can create a transient break on one strand, whereas Type II topoisomerases can produce breaks on both strands. Type IA and II enzymes then allow the unbroken strand(s) to pass through break(s) and rejoin the broken ends; whereas Type IB en-

*To whom correspondence should be addressed. Tel: +1 410 558 8334; Fax: +1 410 558 8331; Email: wangw@grc.nia.nih.gov
Correspondence may also be addressed to Dr. Dongyi Xu. Email: xudongyi@pku.edu.cn

zymes allow swiveling of the broken strand around the intact strand, and then re-ligate the broken ends. As a result, supercoils generated during replication can be relaxed, interlocked DNA rings can be separated, and DNA circles can be interconverted with knots.

Unlike the well-characterized DNA topoisomerases, RNA topoisomerases have received far less attention and their prevalence, function and mechanism of action are largely unknown. To date, only two proteins have been reported to possess topoisomerase activity for RNA–*E. coli* topoisomerase III (EcoTop3) (3) and human topoisomerase 3β (HumTop3β) (4). Both belong to the Type IA family of topoisomerases, hinting that this family may have dual activities for both DNA and RNA. However, two other members of the type IA family from identical species, *E. coli* topoisomerase I (EcoTop1) and human topoisomerase 3α (HumTop3α), lack RNA topoisomerase activity. The reason for this difference remains unclear. For human Top3 paralogs, however, the difference probably involves an RGG box RNA-binding domain that is present only in Top3β but not Top3α. Deletion of this domain strongly reduces the RNA topoisomerase activity of Top3β, suggesting that the domain targets the enzyme to RNA to enable strand passage reactions.

Several lines of evidence suggest that Top3β interacts with other RNA-binding proteins (RBPs) to regulate mRNA translation. First, Top3β forms a stoichiometric complex with TDRD3 (Tudor domain-containing 3), and this complex biochemically and genetically interacts with FMRP (4,5), an RBP that is deficient in Fragile X syndrome and is known to regulate translation of mRNAs important for neuronal function and autism (6). Notably, the interaction between Top3β–TDRD3 complex and FMRP is abolished by a disease-associated FMRP mutation (4); and Top3β gene deletion has also been linked to schizophrenia and intellectual disability (5). Second, Top3β has been reported to bind many mRNAs *in vivo*, and these mRNAs are enriched with known FMRP targets (4). Moreover, the distribution of Top3β-binding sites on mRNAs is similar to that of FMRP—dense in open reading frames and sparse in untranslated regions, again supporting the notion that the two proteins work together in translation (4). Third, Top3β resembles TDRD3 and FMRP in its association with active-translating polyribosomes, and its localization in RNA stress granules, which are aggregations of non-translating mRNAs formed transiently in response to cellular stress (4,7,8). Fourth, Top3β binds multiple mRNAs encoding proteins with neuronal functions related to schizophrenia and autism (4). Expression of one such gene, ptk2/FAK (protein kinase 2/focal adhesion kinase) is reduced in synapses at neuromuscular junctions (NMJs) of Top3β mutant flies. Synapse formation is defective in both flies and mice deleted for Top3β, as observed in FMRP mutant animals. These data suggest that Top3β works with FMRP and TDRD3 to regulate expression of mRNAs important for neurodevelopment and mental health.

Here, we investigate three salient questions regarding RNA topoisomerases: (i) how prevalent are they? (ii) which domains are required for their activity? And (iii) do they associate with polyribosomes as human Topoisomerase 3β does? Our results show that RNA topoisomerase activity is prevalent in Type IA topoisomerases from all domains of life. Moreover, the activity requires the conserved Type IA core domains and the same catalytic residue used in DNA topoisomerase reactions, but does not absolutely require the non-conserved CTD. Finally, RNA topoisomerases from animals associate with polyribosomes, whereas those from bacteria and yeast do not; and this association requires TDRD3, which is present in animals but absent in bacteria and yeast. Our data suggest that RNA topoisomerases are prevalent in all domains of life, and may participate in mRNA translation in animals.

MATERIALS AND METHODS

Cell culture, media, siRNAs and antibodies

Human HEK293 cells were cultured in DMEM supplemented with 10% fetal calf serum at 37°C, 5% CO_2. TDRD3 Smart-Pool siRNA oligos were purchased from Dharmacon. FMR1 siRNA oligos were purchased from Santa Cruz Biotech. Transfections of plasmids and siRNAs were carried out with Lipofectamine 2000 and Lipofectamine RNAiMAX (Invitrogen), respectively, according to the manufacturer's protocols. Chicken DT40 cells were cultured at 39.5°C, 5% CO_2 in RPMI 1640 medium supplemented with 10% fetal calf serum, 1% chicken serum, 10 mM HEPES and 1% penicillin/streptomycin mixture. Transfection was carried out by electroporation using the Amaxa Nucleofector2 in Solution T. For selection of stable clones, growth medium containing G418 (2 mg/ml), puromycin (0.5 μg/ml) or zeocin (0.5 mg/ml) was used. Drosophila melanogaster Schneider line-2 (S2) cells were grown in 10 cm dish in Schneider's Drosophila medium (Gibco) supplemented with 10% FBS and 1% penicillin/streptomycin (Invitrogen) at 25°C inside a normal atmosphere incubator. *Saccharomyces cerevisiae* strain (MATa ade2-1 ura3-1 his3-11, 15 trp1-1 leu2-3, 112 can1-100 Top3-V5::TRP1) was kindly provided by Dr. S. Brill (9). It was grown in YPD medium in an incubator shaker at 28°C and 200 rpm. *E. coli* strains expressing SPA-tagged Top1 (SPA-TopA) and Top3 (SPA-TopB) were kindly provided by Dr. A. Emili (10). They were grown in an incubator shaker at 37°C and 250 rpm.

The anti-RSP-6 antibody was purchased from Cell Signaling Technology (2317s). The Drosophila anti-Top3β antibody was previously described (11). A Drosophila anti-FMRP antibody was purchased from Abcam (ab10299). A human anti-FMRP monoclonal antibody was purchased from Millipore (MAB 2160), and a rabbit anti-cytoskeletal actin antibody (A300-491A) was from Bethyl. Drosophila TDRD3 and Top3β polyclonal antibodies were raised in rabbit against MBP-fused proteins (New England Biolabs) containing a region of TDRD3 (residues 266–323) and Top3β (residues 86–208). The antibodies were affinity-purified using the corresponding immunogen as the affinity matrix. An anti-EcoTop1 monoclonal antibody was generated as described (12). An anti-EcoTop3 polyclonal antibody was a kind gift from Dr. K. Marians (13).

Generation of chicken DT40 knockout cells

Chicken TDRD3-knockout constructs were generated as previously described (14) using MultiSite Gateway Three-Flagment Vector Construction Kit. The 5′ and 3′ arms were amplified from genomic DNA using the primers GGGGACAACTTTGTATAGAAAAGTTG GTAATGGCTAAAGCCAGACCTCATTC/GGGG ACTGCTTTTTTGTACAAACTTGCACCATGAAG CAAACGCACTAC and GGGGACAGCTTTCTTG TACAAAGTGGCGTAAAGCATAACATGTTGGCT GTGAAC/GGGGACAACTTTGTATAATAAAGT TGATATCCACCCAGTAACATTCATTCATCAATG, respectively. These arms were cloned into pDONR P4-P1R and pDONR P2R-P3 vectors, respectively. The knockout constructs were generated by LR recombination of pDONR-5′ arm, pDONR-3′ arm and resistant gene cassettes-contained pDONR-211. The knockout constructs were linearized by digestion with EcoRV restriction enzyme before transfection into DT40 cells. The primers GAAGGTTGTCAATCCATGGAACTGGAG/GCCT TGCTAAGTCTGACTCAGCAGACAG were used for genomic DNA PCR to identify knockout clones.

Generation of Drosophila Tdrd3-knockout S2 cells

Drosophila tdrd3 CRISPR targeting S2 stable cell lines were generated as described by Bassett et al. and O'Connor-Giles (15,16). To summarize, forward (TTCGGAGAGACCAC CGCGAGAGCG) and reverse (AACCGCTCTCGCGG TGGTCTCTCC) primers were selected from the CRISPR optimal target finder (http://tools.flycrispr.molbio.wisc.edu/targetFinder/). Two phosphorylated oligos (10 μM) in a mixture containing NEB T4 ligation buffer were heated to 95°C and the annealing process occurred after gradually cooling the mixture to 25°C. The pAc-sgRNA-Cas9 vector was obtained from Addgene (plasmid # 49330) and digested with BspQ1. The linearized vector was ligated using the annealed oligo insert and transformed into GC10 competent cells (Sigma). Sequencing confirmed the correct inserts.

For transfection, 2 μg of CRISPR plasmid was transfected in 2×10^6 of S2 cells cultured in Schneider's medium (Gibco) with 10% fetal bovine serum (FBS) at 25°C using Fugene HD transfection reagent (Promega). Transfections were performed in six-well plate. After 3 days, puromycin was added to final concentration of 5 μg/ml, and cells were transferred to 10 cm dish. After 4 days, cells were transferred to four 96-well plates at different dilutions. Once the cells reached confluency, they were collected, and the genomic DNAs were amplified using primers (GATAATAGTATGCACCGTCAGCCGA) and (AGAT TCAGTTGGGGAACTGGCT), followed by sequencing. Western blotting was used to screen the absence of TDRD3 protein in the knockout cells.

Expression and purification of recombinant topoisomerases from different species

Recombinant EcoTop1 wildtype and mutant proteins were expressed and purified as described (17). Recombinant Mycobacterium topoisomerases were expressed and purified as described (18). NeqTop3 and its mutant were expressed and purified as described (19). TmaTop1 was expressed and purified as described (20). SsoTop3 was purified as described (21). His-tagged Yeast Top3 and Top3-Rmi1 complex were expressed and purified as described before (22). MBP-Top3 and MBP-top3-Y356F were also expressed and purified similarly, except that amylose resin was used at the affinity purification step instead of Ni-NTA resin. A recombinant reverse gyrase from *S. solfataricus* was expressed and purified as described (23,24). A recombinant reverse gyrase from *N. equitans* was expressed and purified as described (25,26).

Expression and purification of human Top1 and Top1mt from Baculovirus-infected insect cells were performed as previously described (27). Briefly, His-tagged Top1 or Top1mt expression vector was packaged into Baculovirus. Then, Sf9 cells (1 liter) were infected with an MOI (Multiplicity of infection) of 3, incubated at 27°C and harvested at 48 h post-infection. The cell pellet from Baculovirus-infected insect cells was re-suspended with 10 volumes of extraction buffer (final concentration of 20 mM HEPES, pH 7.3, 300 mM NaCl, 5 mM $MgCl_2$, 5% glycerol, 2 mM β-mecaptoethanol, 80 mM imidazole) and complete protease inhibitors as per the manufacturer's instructions (Roche) per gram wet weight. The sample was sonicated to lyse the cells, clarified by centrifugation at 111 000 × g for 50 min, filtered (0.45 μm) and applied to a 5 ml His-Trap column (GE Healthcare) equilibrated with extraction buffer. The column was washed with extraction buffer to baseline, and proteins were eluted over a 20 column volume gradient with extraction buffer at 1 M NaCl and 1 M imidazole. Samples were dialyzed twice for at least 4 h at 4°C against at least 20 sample volumes of final buffer using 10K MWCO Snakeskin (Pierce) dialysis membrane or Slide-A-Lyzer (Pierce) cassettes.

The recombinant Variola DNA topoisomerase was expressed in *E. coli* strain BLR (DE3) containing plasmid pET21a(+)-vTop. The *E. coli* was grown in LB in the presence of 50 μg/ml of ampicillin. When OD600 reached ∼0.5, the expression of Variola DNA topoisomerase was induced by adding 1 mM of IPTG. The recombinant Variola DNA topoisomerase was purified by an SP-Sepharose FF column and followed by a Nickel affinity column.

HumTop1 and HumTop2α were purchased from TopoGEN Inc. Two different sources of humTop1 showed results that are indistinguishable.

Cloning and expression of humTop3β variants

For generating CTD-deletion mutant of humTop3β (ΔCTD), the whole N-terminal sequence was PCR amplified from pcDNA-His-Flag-humTop3β using forward primer, AAAAAGCTTg**CCACCAT***g***gACTACAAggAC gACgATgACAag**ATGAAGACTGTGCTCATGGTTG (HindIII restriction site is underlined, Kozak sequence is underlined and bold letters, and flag sequence is in bold letters), reverse primer AAAGAATTCTCAGCGTGAG AGGGGCTTGCC (EcoR1 restriction site is underlined), and AccuPrime™PfxSuperMix polymerase (Invitrogen) as per manufacturer's protocol. The product was cloned into pCDNA3 vector between HindIII and EcoR1 restriction sites.

Flag-tagged human Top3β and its mutant were expressed and purified as described previously (4). Briefly, HEK 293 cells were transfected with pcDNA constructs of human Top3β and its mutant using polyethylenimine (PEI). Cells were incubated in CO_2 incubator shaker at 130 rpm, 5% CO_2 for 72 h. Cells were then harvested, washed 2 times with cold PBS, and lysed in 3.5 volume of lysis buffer containing 20 mM Tris pH 7.5, 500 mM NaCl, 10% glycerol, 0.5% NP40, 10 mM NaF and protease cocktail (Roche) on ice for 30 min. Two volumes of cold 20 mM Tris pH 7.5 was added to the cell lysate, and the diluted lysate was centrifuged at 18 000 rpm at 4°C for 30 min. The supernatant was incubated with the anti-Flag M2-agarose beads (Sigma) at 4°C for 3 h. Beads were washed three times with cold washing buffer (50 mM Tris pH 7.5, 500 mM NaCl, 10% glycerol, 0.5% NP40, 1% EDTA and protease inhibitor cocktail), and once with cold elution buffer (25 mM Tris pH 7.5, 100 mM NaCl and 10% glycerol) for 5–8 min per wash. Flag-tagged proteins were eluted from anti-Flag M2 agarose beads in elution buffer with 200 μg/ml 3× Flag peptide (Sigma).

RNA topoisomerase assay

The circular RNA substrate was generated and purified as described (4). Briefly, two oligos, K128f and K128r were annealed and the double stranded product was used as a template for transcription of 128 bases long single stranded RNA (GGGAGAUUUUUUUUUU UUUUUUUUUUGUCAGACGGAUCUUUUUUUU UUUUUUUUUUUUUCUCCCGACUGGUUUUUU UUUUUUUUUUUUUUUGAUCCGUCUGACUUUU UUUUUUUUUUUUUU UUCCAGUC). Transcription was performed using MEGAshortscript™ T7 kit (Ambion) as per manufacturer's protocol. RNA was purified from 6% TBE urea gel (Invitrogen) after 45 min electrophoresis at 180 V. Purified RNA was labeled with (γ^{32}) ATP (PerkinElmer) using KinaseMax kit (Ambion) following the manufacturer's protocol.

For generation of circular RNA, 4 μM of the above ^{32}P labeled RNA was annealed with 20 μM DNA oligo K128link (4) in a buffer containing 10 mM Tris pH 7.5, 100 mM NaCl in a 15 μl reaction mixture for 2–3 h. T4 RNA ligase (Ambion) was added to the annealed product and incubated for 3 h at 37°C in a 20 μl reaction mixture. DNA was removed by treating the reaction with 4 units TURBO DNase (Ambion) for 15 min at 37°C. The circular RNA substrate was purified from 15% TBE–urea gel (Invitrogen) after 11–12 h electrophoresis at 150 V.

The stand passage reaction was set up as described (4). Briefly, 1 nM or 3000 cpm of RNA circle was incubated with indicated protein concentrations in a 10 μl reaction mixture containing 10 mM Tris pH 7.5, 5 mM $MgCl_2$, 2 mM DTT, 0.1 mg/ml BSA, 5% glycerol, 10% PEG400 and 4 units RNaseOut (Invitrogen) at 37°C for 90 min. The reaction was terminated using 2 μl 5× stop buffer (1% SDS, 100 mM EDTA and 1 mg/ml proteinase K (Ambion). The resulting substrates were resolved on 15% TBE–urea gel after 6 h electrophoresis at 150 V and analyzed by Storm 860 molecular imager (Molecular Dynamics). RNA topoisomerase assay reaction for TmaTop1 and NeqTop3 was incubated at 50°C. In RNA topoisomerase reaction using reverse gyrase proteins, 1 mM ATP was also included into the reaction buffer. Phenol:choloroform:isoamylalcohol was used to stop the reaction and distinguish the RNA knot from the RNA-protein complex which produces a gel-shift with distinct mobility compared to the RNA knot. It should be mentioned that we cannot convert more than 33% of the circles to knots in our assay. There are at least two possible explanations. First, the topoisomerase can convert not only a circle to a knot, but also a knot to a circle (3). Because the topoisomerase assay used here is a reversible reaction, the extent of the reaction is determined by not only the forward reaction rate, but also the reverse reaction rate. When large amounts of circles are converted to knots, the reverse reaction rate may become larger than the forward reaction, until the reaction reaches an equilibrium. Second, only about 33% the circular substrates may be folded correctly to allow knot formation, whereas the other substrates may be folded into conformations that prevent knot formation.

Polyribosome assay

The polyribosome assay for human HEK293 cells was done as described (4). The assay for Drosophila S2 Cells, chicken DT40 cells, and bacteria topoisomerases were performed as described (28–30).

Generation of phylogenetic tree

The phylogenetic trees for Top3β, TDRD3 and FMRP were generated using the pSI-BLAST tool from the NCBI website:

(http://blast.ncbi.nlm.nih.gov/Blast.cgi?PROGRAM=blastp&PAGE_TYPE=BlastSearch&LINK_LOC=blasthome). Top3β and TDRD3 were only detected in eukarya by the BLAST search, and their trees were built using only search data from eukarya. FMRP was detected only in animals by BLAST search, and its tree was built using search data only from animals.

RESULTS

E. coli topoisomerase I has RNA topoisomerase activity

We screened published DNA topoisomerases from bacteria, archaea and eukarya for RNA topoisomerase activity. We started with Type IA topoisomerases because they are the most ubiquitous topoisomerases present in nearly all species. The prototype of this family is EcoTop1, which is the first DNA topoisomerase discovered (1,2). Notably, EcoTop1 was reported to lack RNA topoisomerase activity using assays that interconvert a single-strand (ss) RNA between two different topological forms: a circle and a knot (3) (Figure 1A). This feature differs from that of its paralog, EcoTop3, which displays RNA activity in the same assays. We found these results puzzling because the two *E. coli* topoisomerases share high degrees of sequence and structure similarity in their catalytic core domains (Toprim and domains II–IV) (31). We therefore re-examined EcoTop1 in an RNA knotting assay previously employed by our group, which shows that humTop3β can convert an ssRNA circle to a knot (4) (Figure 1A). Our ssRNA substrate is similar to that described by Seeman and colleagues, two pairs of

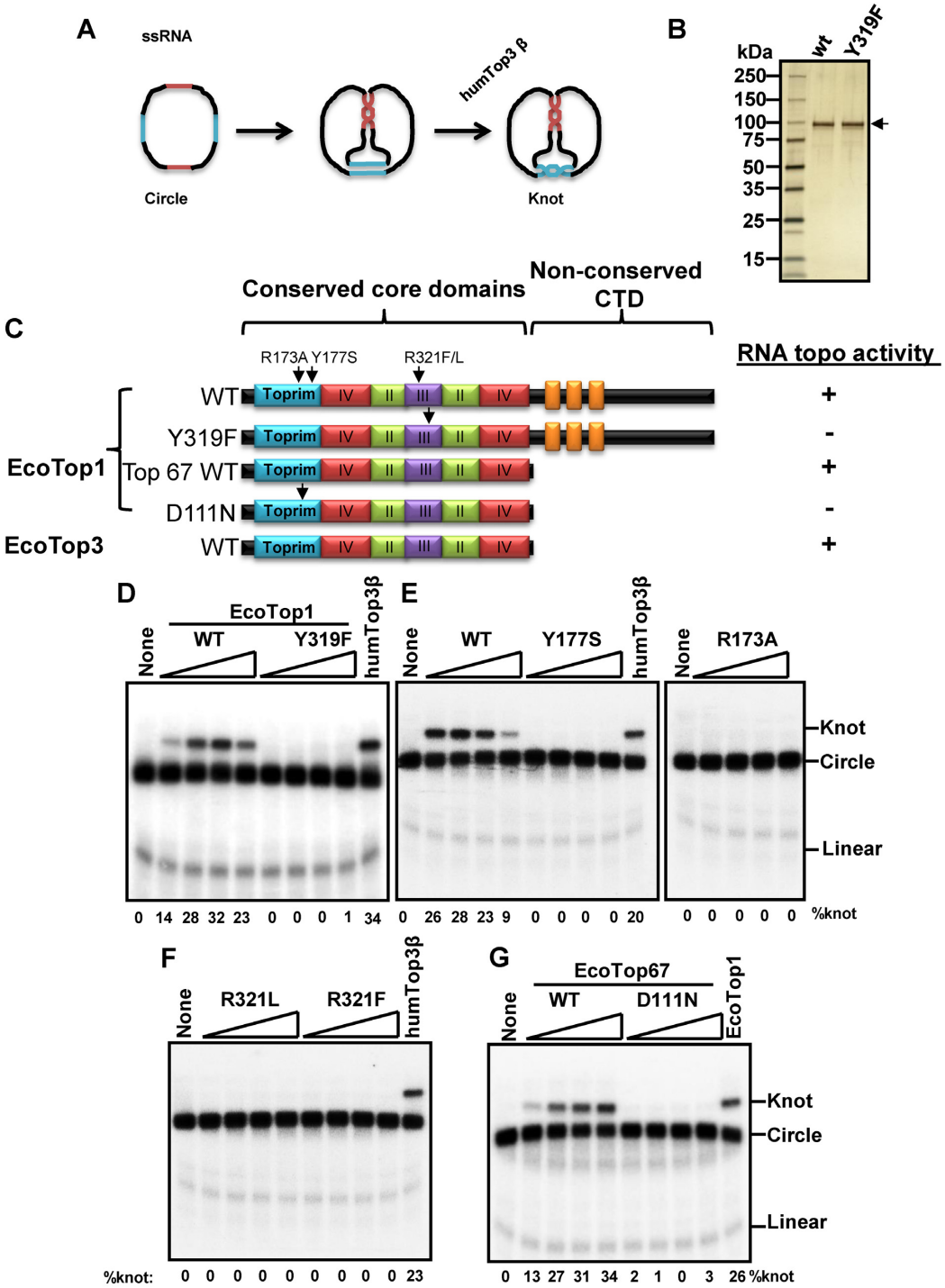

Figure 1. *E. coli* Topoisomerase I has RNA topoisomerase activity that depends on the conserved Type IA core domains but not the non-conserved CTD. (**A**) Schematic representation of RNA topoisomerase assay (4). A 128-base long synthetic circular RNA contains two pairs of complementary region (Red and blue) separated by single-stranded spacer region (black). The circular substrate is converted to knot after strand passage reaction where the two pairs of complementary regions form double helices. (**B**) A silver-stained SDS gel showing purified recombinant wild-type (wt) or Y319F mutant EcoTop1. (**C**) Schematic representation of EcoTop1 wildtype and various mutants; and EcoTop3 and its mutant. The conserved core domains and the non-conserved CTDs, including Zn-fingers (orange boxes), are indicated. Their RNA topoisomerase activity was shown on the right. Arrows show the location of point mutation in the respective domain. (**D**) Autoradiograph from RNA topoisomerase assay showing that EcoTop1, but not its catalytic mutant Y319F, has RNA topoisomerase activity. The reaction mixture contains increasing concentrations (2.5, 5, 10 and 20 nM) of proteins. The percentage of the knot product in total RNA (circle and knot) is shown below each lane. (**E**, **F**) RNA topoisomerase assay showing wild type EcoTop1, but not its mutants as indicated, has RNA topoisomerase activity. The reaction mixture contains increasing concentrations (2.5, 5, 10 and 20 nM) of proteins. 4 nM of humTop3β was used as positive control. (**G**) RNA topoisomerase assay showing that the CTD-deletion mutant of EcoTop1, EcoTop67, but not its point mutant, D111N, has RNA topoisomerase activity. The reaction mixture contains increasing concentration (7.5, 15, 30,and 60 nM) of proteins. 10 nM of full-length EcoTop1 was used as positive control.

complementary regions separated by single-stranded spacers (3) (Figure 1A). When one complementary region forms a duplex, the other region requires a strand-passage reaction to form a stable duplex. However, one important difference is that our substrate has complementary regions of 12 bp, which are longer than the 10 bp used in Seeman's study. The longer complementary regions should further stabilize the duplex and make the strand-passage reactions thermodynamically more favorable.

Using this assay, we found that the purified EcoTop1 wild type (WT) protein (Figure 1B and C) converted the RNA circle to knot with conversion efficiency similar to that of humTop3β (32% vs. 34%) (Figure 1C and D), indicating that EcoTop1 possesses RNA topoisomerase activity. An EcoTop1 mutant carrying substitution of the catalytic Tyr residue by Phe (Y319F; Figure 1B and C) showed no detectable activity (Figure 1C and D), suggesting that EcoTop1 may use the same Tyr residue to catalyze reactions on both DNA and RNA.

We noticed that at increasing concentrations of EcoTop1, the RNA topoisomerase activity was first increased and then decreased (Figure 1D). This feature is shared by many other topoisomerases (see below). One possibility is that too much topoisomerases may coat the ssRNA substrate to prevent strand passage reactions.

The conserved type IA core domain of EcoTop1 is necessary and sufficient for RNA topoisomerase activity

Previous studies have shown that EcoTop1 requires both its conserved core domains and the divergent C-terminal domain (CTD) for its DNA topoisomerase activity in supercoiled DNA relaxation assay (32). We investigated which of these domains is needed for EcoTop1 RNA topoisomerase activity. We first examined several point mutants within the conserved core domains of EcoTop1, including Y177S and R173A (Figure 1C), which are defective at both DNA cleavage and rejoining steps of the strand passage reaction (33); as well as R321L and R321F (Figure 1C), which are deficient at the rejoining step (17). All of these mutants were deficient in the RNA strand-passage assay (Figure 1E and F), indicating that EcoTop1 requires its conserved core domains to catalyze topoisomerase reactions for both DNA and RNA.

We next investigated the importance of the CTD domain in EcoTop1, which has been shown to bind single-stranded DNA and can recognize accumulation of negative supercoils in duplex DNA (34,35). A 67-kDa EcoTop1 mutant protein with deletion of its CTD (Top67-WT) (Figure 1C) lacks DNA relaxation activity (36) but retains DNA catenation activity (34), indicating that the CTD is specifically needed for removal of supercoils in duplex DNA but not absolutely essential for strand-passage. In our assay, this mutant protein converted the RNA circle to a knot as efficiently as the full-length protein (Figure 1G; about 30%). As a control, the same 67-kDa protein carrying a point mutation within the core domains, D111N, which is defective at the rejoining step of DNA passage reaction (37), failed to convert any detectable amount of the RNA circle to knot (Figure 1G). Thus, the CTD of EcoTop1 is dispensable for RNA topoisomerase activity, and the conserved core domains are both necessary and sufficient for RNA topoisomerase of EcoTop1. Moreover, the CTD and its associated binding activity for nucleic acids are dispensable for strand passage reactions by either DNA or RNA.

E. coli and human RNA topoisomerases have different requirement of their CTDs

The results that the conserved core domains are sufficient for the RNA topoisomerase activity of EcoTop1 prompted us to test whether these domains are also sufficient for RNA topoisomerase activity of humTop3β. We constructed a humTop3β mutant (ΔCTD) deleted of its entire CTD, which consists of four C4 Zn-finger motifs and an RNA binding motif (RGG box) (Supplementary Figure S1A and S1B). This mutant failed to convert any detectable RNA circles to knots (Supplementary Figure S1C and S1D). The data are consistent with our earlier findings that humTop3β deleted of RGG box alone has significantly reduced RNA topoisomerase activity (4). Together, these data suggest that unlike EcoTop1, human Top3β requires both core domains and CTD for RNA topoisomerase activity.

RNA topoisomerase activity is present in several Type IA topoisomerases from all three domains of life

Screening Type IA topoisomerases from other bacteria (Figure 2A) revealed that topoisomerase I (TmaTop1) from *Thermotoga maritima*, a hyperthermophilic bacterium that grows at 80°C (38), efficiently converted the RNA circle to knot at either 37 or 55°C, with the conversion efficiency higher at the latter temperature (Figure 2B and C). In contrast, topoisomerase I from *Mycobacterium tuberculosis* and *Mycobacterium smegmatis* (39) failed to convert any amount of the RNA circle to knot (Figure 2B and D). Combined with the findings from *E. coli*, the data suggest that RNA topoisomerase activity is present in some but not all Type IA topoisomerases from bacteria.

To date, no RNA topoisomerase activity has been detected in proteins from archaea. We found that topoisomerase 3 from two archaeal species, *Nanoarchaeum equitans* (NeqTop3) (19) and *Sulfolobus solfataricus* (SsoTop3) (40) (Figure 3A–C), exhibited RNA topoisomerase activity similar to that of humTop3β (Figure 3A, D and E), indicating that the activity is present in this domain of life. Moreover, NeqTop3 carrying a point mutation of the catalytic Tyr residue (NeqTop3-Y293F) lacked such activity (Figure 3B and D). These data support the notion that all Type IA topoisomerases use the same conserved Tyr residue to catalyze both DNA and RNA strand passage reactions. Our screening also revealed that two reverse gyrases from archaea, which contain both Type IA core domains and a helicase-like domain (24,25), lacked RNA topoisomerase activity (data not shown).

We have previously identified humTop3β as the first RNA topoisomerase in eukaryotes (4). Because human represents a multicellular eukaryote, we examined the budding yeast *Saccharomyces cerevisiae*, a unicellular eukaryote containing only one Type IA enzyme–yTop3 (Figure 4A) (2). We expressed and purified recombinant yTop3 proteins fused to either Maltose-binding protein (MBP) or 6-histidine tags (His) from *E. coli* (Figure 4B), and found that

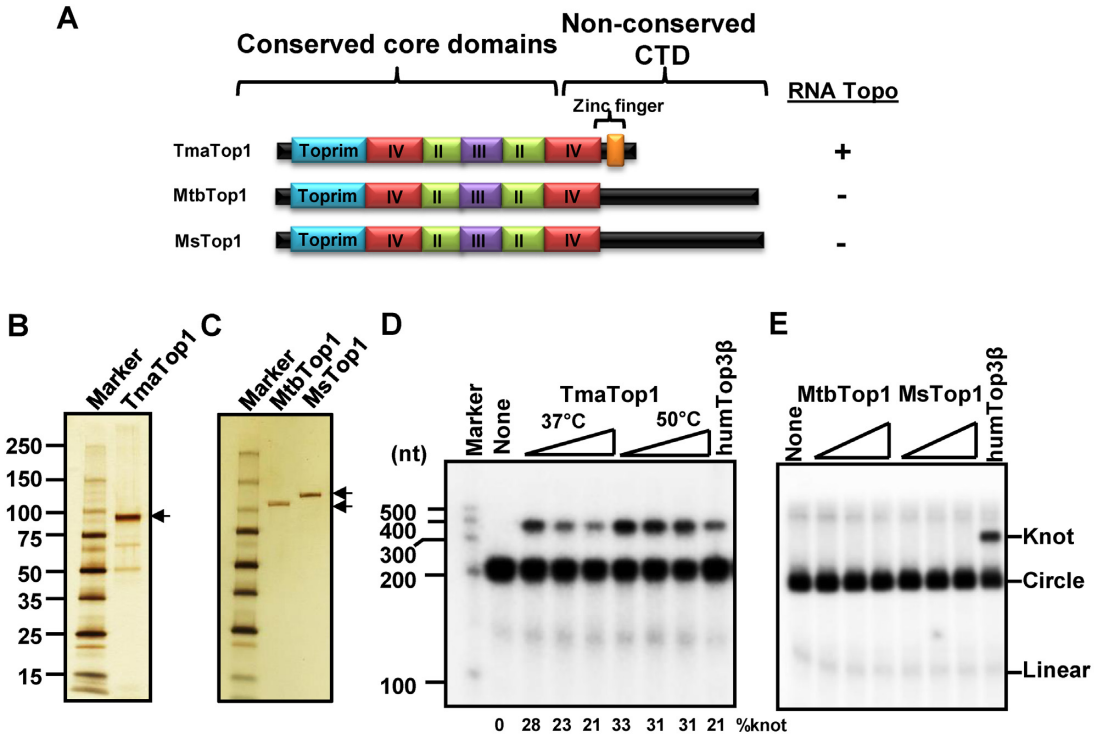

Figure 2. RNA topoisomerase activity is present in some but not all bacterial Type IA topoisomerases. (**A**) Schematic representation of RNA topoisomerase representatives from bacteria. The conserved core domains and the non-conserved CTDs, including a Zn-finger (an orange box), are indicated. Their RNA topoisomerase activity was summarized on the right. (**B**) Silver-stained SDS gels showing purified recombinant *Thermotoga maritima* Top1 (TmaTop1), *Mycobacterium tuberculosis* Top1 (MtbTop1), and *Mycobacterium smegmatis* Top1 (MsTop1). (**C**) Autoradiograph from RNA topoisomerase assay showing TmaTop1 can convert the circular RNA substrate into a knot. The reaction mixtures contain increasing concentrations (2, 4, and 8 nM) of TmaTop1 at 37°C or 50°C. (**D**) An autoradiograph from RNA topoisomerase assay shows that MtbTop1 and MsTop1 (5, 10 and 20 nM) has no detectable RNA topoisomerase activity. 4 nM humTop3β was used as a positive control.

both proteins catalyzed conversion of the RNA circle to knot (Figure 4C and D). The His-tagged yTop3 appears to have higher conversion efficiency (Figure 4D), which could be due to the fact that smaller tag that may interfere less with the reaction. The MBP-fused yTop3 carrying a point mutation of its catalytic residue (Y356F) failed to catalyze the conversion (Figure 4C). The data suggest that the RNA topoisomerase activity may be conserved from yeast to human, and requires the same Tyr residue for catalysis.

It has been shown that yeast Top3 associates with Rmi1 to form a complex that has DNA topoisomerase activities *in vitro* (22,41) and suppresses recombination *in vivo* (9,42). We expressed and purified recombinant His-tagged yeast Top3-Rmi1 complexes from *E. coli*, and found that this complex catalyzed conversion of the RNA circle to knot at efficiency comparable to that of the yTop3 alone (Figure 4D). The data suggest that Top3-Rmi1 complex has both DNA and RNA topoisomerase activity, and Rmi1 does not appear to play a major catalytic role.

Type IB topoisomerases are known to catalyze relaxation of supercoiled DNA by a swiveling mechanism (43); but they are also capable of catalyzing strand passage reactions, including catenation (44). In addition, several Type IB topoisomerases can cleave ribonucleotides incorporated in DNA (45,46), hinting that they may have RNA topoisomerase activity. Our screening showed that three Type IB DNA topoisomerases, human topoisomerase I (Top1) (47), human mitochondrial topoisomerase (Top1mt) (48), and Variola virus topoisomerase (49) failed to convert the RNA circle to knot (Supplementary Figure S2A-C). However, we cannot exclude the possibility that these enzymes may relax supercoiled dsRNA similar to their actions on dsDNA.

Type II DNA topoisomerases can also cleave ribonucleotides incorporated in DNA (50), implying that they may possess RNA topoisomerase activity. However, because these enzymes act by simultaneously cleaving and rejoining both strands of DNA duplex, they are not expected to act on the ssRNA circle substrate used in our assay. As expected, a Type II DNA topoisomerase, humTop2α, failed to convert any detectable amount of ssRNA circle to knot (Supplementary Figure S2D). Future experiments with dsRNA substrates are needed to examine RNA topoisomerase activity for these enzymes.

Top3β homologs from animals associate with polyribosomes

We and others have previously shown that human Top3β, along its interacting partners TDRD3 and FMRP, associate with polyribosomes (4,5), suggesting that Top3β may mediate mRNA translation together with its partners. Because RNA topoisomerase activity is prevalent in Type IA topoisomerases from all three domains, we investigated whether the polyribosome association is a feature conserved in these enzymes.

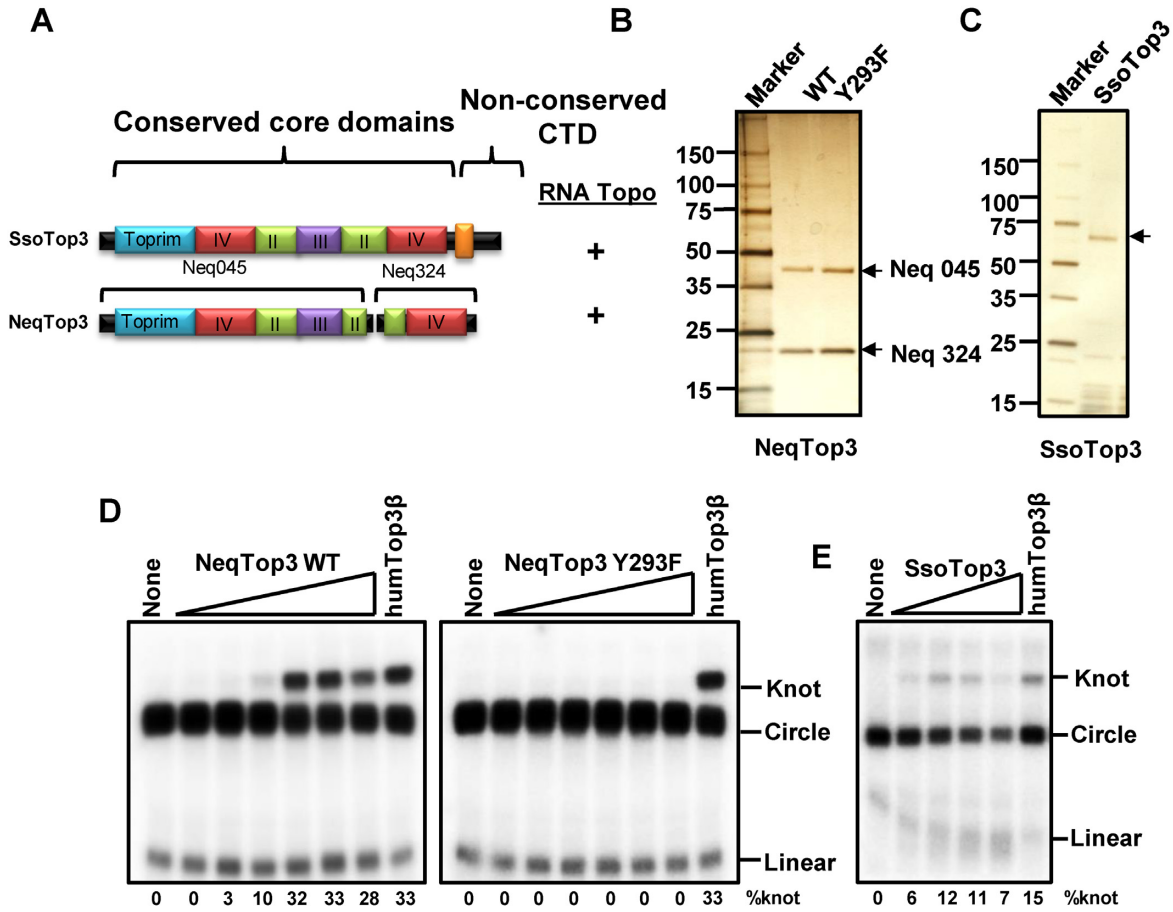

Figure 3. RNA topoisomerase activity is present in several archaeal Type IA topoisomerases. (**A**) Schematic representation of *Nanoarchaeum equitance* topoisomerase 3 (NeqTop3) and *Sulfolobus solfataricus* topoisomerase 3 (SsoTop3). The conserved core domains and the non-conserved CTDs, including a Zn-finger (an orange box), are indicated. Their RNA topoisomerase activity was shown on the right. (**B**, **C**) A silver-stained SDS gel showing purified recombinant wt NeqTop3, its catalytic mutant Y293F and SsoTop3. (**D**, **E**) RNA topoisomerase assay showing that two Type IA enzymes from archaea, NeqTop3 (**D**) and (SsoTop3) (**E**), can convert the circular RNA substrate into knot, whereas NeqTop3-Y293F mutant lacked the activity. The reactions include increasing concentrations (0.62, 1.25, 2.5, 5, 10 and 20 nM) of NeqTop3-wildtype and its catalytic mutant Y293F; and SsoTop3 (1.25, 2.5, 5.0 and 10 nM) at 50°C. The percentage of the knot product in total RNA (circle and knot) was indicated below each lane. Four nM humTop3β was as positive control.

We first tested Drosophila Top3β, which has previously been shown to resemble human Top3β in association with TDRD3 and FMRP (4). Sucrose-gradient fractionation of Drosophila S2 cell lysate followed by immunoblotting revealed that a subset of Top3β, TDRD3 and FMRP were present in the polyribosome fractions (Figure 5A; Supplementary Figure S3A). To verify that their presence in these fractions is due to polyribosome association, we treated S2 cell lysate with EDTA, which is known to disrupt polyribosomes, prior to the fractionation step. As expected, the EDTA pretreatment strongly disrupted polyribosomes, as evidenced by reduced levels of RNA (as measured by OD_{260}) as well as a ribosomal protein (RPS6) in the polyribosome fractions (Figure 5A and Supplementary Figure S3A). Notably, the treatment also reduced the levels of Top3β, TDRD3 and FMRP in the same fractions (Figure 5A), indicating that the Drosophila Top3β-TDRD3-FMRP complex associates with polyribosomes similarly as the human complex.

We next analyzed Top3β-polyribosome association in chicken DT40 cells. Similar to the findings in human and Drosophila cells, a subset of Top3β, TDRD3 and FMRP in DT40 cells co-fractionated with polyribosome fractions as revealed by immunoblotting of sucrose gradient fractions of cell extracts (Figure 5B; Supplementary Figure S3B). Moreover, the levels of these proteins in the polyribosome fractions were reduced by EDTA treatment prior to the fractionation. The data indicate that the polyribosome association is conserved for chicken Top3β complex.

We subsequently performed the assay for the Top3β homolog in yeast, Top3. Although a fraction of Top3 was detected in the high-molecular-weight sucrose fractions, this level was unaltered by EDTA treatment (Supplementary Figure S4A and S4B). The control experiment shows that the EDTA treatment disrupted the polyribosomes (Supplementary Figure S4B). These data indicate that yeast Top3 does not associate with polyribosomes, but may be part of some high-molecular-weight complexes that are resistant to EDTA.

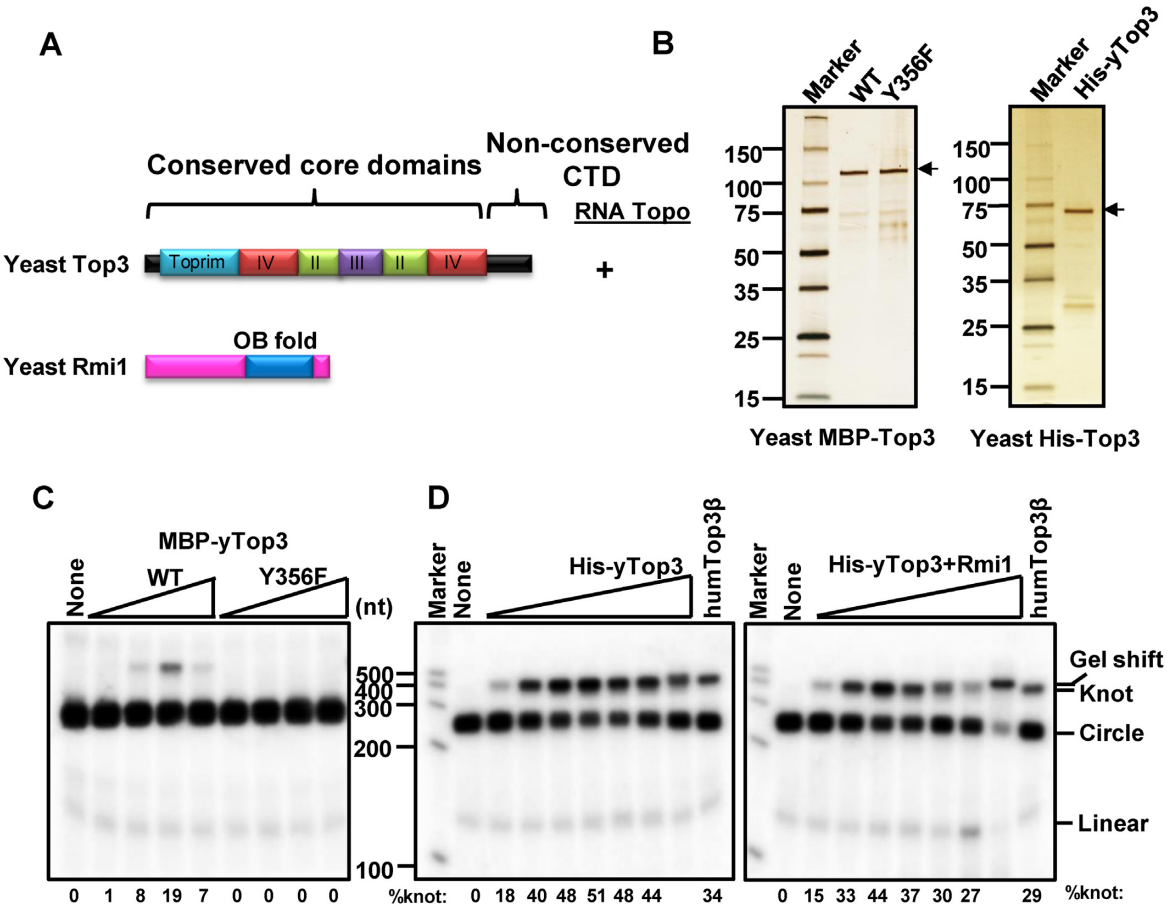

Figure 4. The Type IA topoisomerase from yeast *Saccharomyces cerevisiae* has RNA topoisomerase activity. (**A**) Schematic representation of Top3 of *Saccharomyces cerevisiae* (yTop3) and its partner, Rmi1. The conserved core domains and the non-conserved CTDs of yTop3 are indicated. The OB fold of Rmi1 is indicated in dark blue color. The RNA topoisomerase activity was shown on the right. (**B**) Silver-stained SDS gels showing purified recombinant MBP-yTop3, its catalytic mutant Y356F, and 6-Histidine tagged wildtype yTop3 (His-yTop3). (**C**) RNA topoisomerase assay showing that MBP-yTop3 but not its catalytic mutant Y356F, has RNA topoisomerase activity. The reaction mixture contains increasing concentrations (2.5, 5, 10 and 20 nM) of wildtype or Y356F mutant of MBP-yTop3. (**D**) RNA topoisomerase assay showing that yTop3-Rmi1 complex has similar activity as yTop3 alone. The reaction mixture contains increasing concentration (0.8, 1.6, 3.1. 6.2, 12.5, 25 and 50 nM) of his-tagged yTop3 (left) or yTop3-Rmi1 complex (right). At 50 nM concentration, His-tagged yTop3 proteins stably bound the RNA substrate to produce a gel-shift band with distinct mobility compared to knot. The gel-shift band can also be distinguished from knot by phenol-chloroform treatment, which abolishes the gel-shift band but does not affect the band corresponding to an RNA knot (data not shown). 4 nM humTop3β was used as a positive control.

We also examined polyribosome association for Top3β homologs in bacteria *E. coli*, EcoTop1 and EcoTop3, but failed to observe any association (Supplementary Figure S4C-F). Together, these data suggest that Top3β homologs from animals associate with polyribosomes, whereas those from yeast and bacteria do not.

Top3β homologs in animals require TDRD3 for polyribosome association

We investigated the question of why only Top3β homologs from animals associate with polyribosomes. We hypothesize that Top3β may require its interacting partner, TDRD3, to associate with polyribosomes; and this can only occur in multicellular eukaryotes because TDRD3 is absent in bacteria and yeast by BLAST searches of NCBI database (data not shown) (7,51). In support of this hypothesis, TDRD3 has been shown to be required for Top3β to associate with polyribosomes in a human cancer cell line that lacks TDRD3 (5).

We tested this hypothesis using human HEK293 cells, in which we have previously shown that Top3β, TDRD3 and FMRP associate with polyribosomes (4). We found that in the same cell line depleted of TDRD3 by an siRNA oligo, the levels of both Top3β and TDRD3 were concomitantly decreased in the polyribosome fractions; whereas that of FMRP was largely unaffected, compared to cells treated with a control oligo (Figure 6A, top and middle panels). As a comparison, we also depleted FMRP in the same cell line, and found that the levels of Top3β and TDRD3 in the polyribosome fractions were unchanged (Figure 6A, top and bottom panels). These data suggest that human Top3β requires TDRD3 but not FMRP to associate with polyribosomes.

To determine whether TDRD3 is required for Top3β to associate with polyribosomes in other animals, we inactivated this gene in chicken DT40 cells by gene-targeting

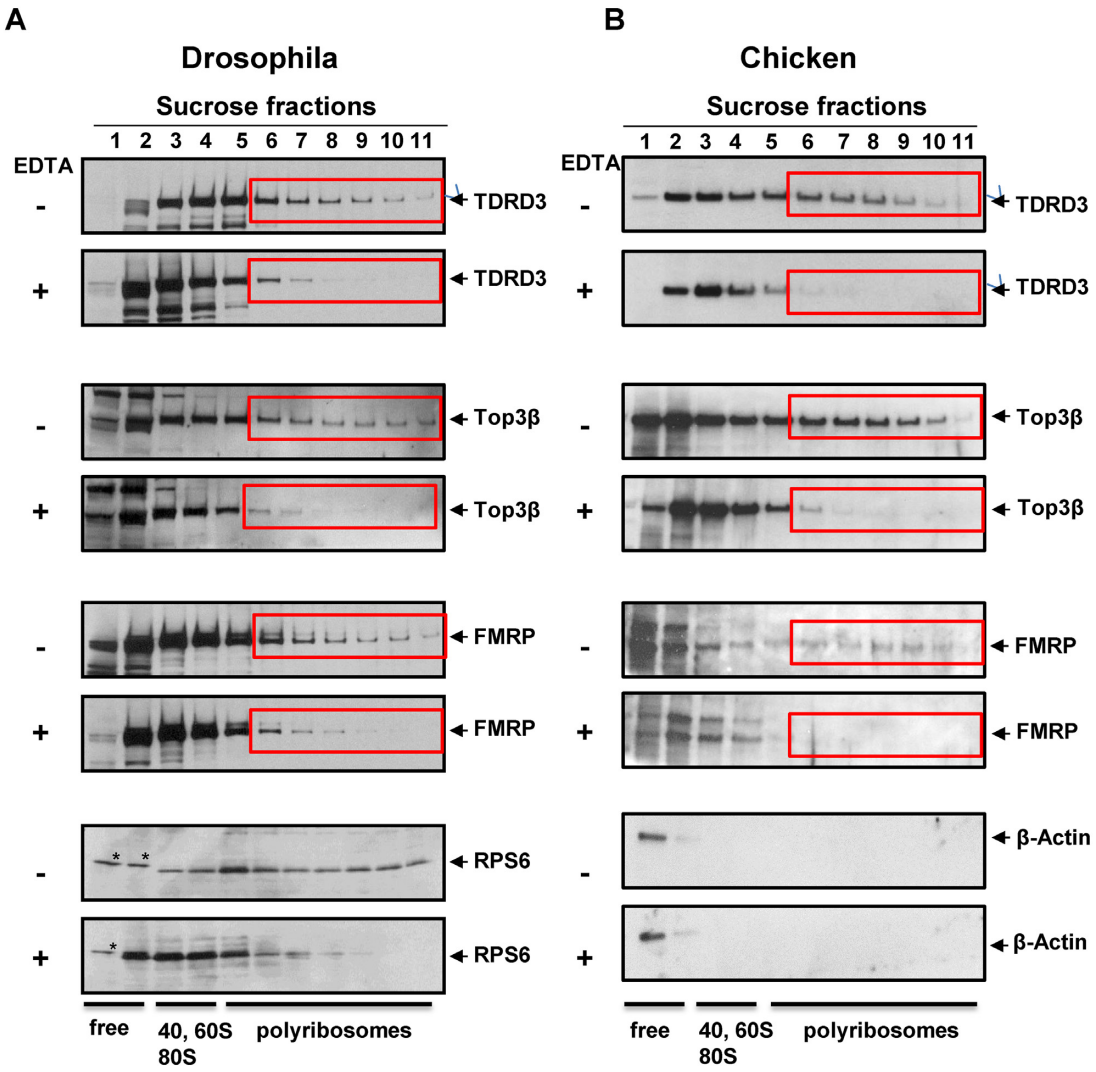

Figure 5. The RNA topoisomerase Top3β associate with polyribosomes in Drosophila and chicken cells. (**A**) Immunoblotting analysis of sucrose fractions of Drosophila S2 cell extracts shows co-sedimentation of Top3β, TDRD3 and FMRP with polyribosomes. Cytoplasmic extracts of S2 cells were prepared and treated with and without EDTA, which is known to disrupt polyribosomes. The absence or presence of EDTA is indicated on the left. Lysates were centrifuged on a 15–60% (w/w) linear sucrose gradient. The presence of ribosomal subunits, mono and polyribosomes was monitored at 254-nm absorption (Supplementary Figure S3A), and indicated as the bottom of the blots. Notably, the co-sedimentation of the above proteins with polyribosome fractions was strongly reduced by EDTA treatment, suggesting that these proteins associate with polyribosomes. (**B**) Immunoblotting analysis of sucrose fractions of chicken DT40 cell lysates shows that chicken Top3β, TDRD3 and FMRP associate with polyribosomes. RPS6, a small ribosomal subunit, was included as a marker for ribosomes. β-actin was included as a negative control, which was absent in polyribosome fractions. The asterisk indicates a polypeptide cross-reactive with RSP6 antibody. The red boxes highlight polyribosome fractions in which the indicated proteins display differences or no changes.

(Supplementary Figure S5A-C). We found that the level of Top3β in the polyribosome fractions was reduced in *TDRD3*$^{-/-}$ DT40 cells compared to wildtype cells (Figure 6B, top and middle panels); and this reduced level was recovered when human TDRD3 was ectopically expressed in the same cells (Figure 6B, middle and bottom panels). In comparison, the level of FMRP in polyribosome fractions was largely unaffected in *TDRD3*$^{-/-}$ DT40 cells. The data suggest that TDRD3, but not FMRP is required for Top3β to associate with polyribosomes in vertebrate cells.

To extend the study to invertebrate cells, we inactivated TDRD3 gene in *Drosophila* S2 cells using CRISPR-Cas9 technology (15,16), and confirmed the gene inactivation by genomic sequencing and immunoblotting (Supplementary Figure S6). Notably, the signal of Top3β in polyribosome fractions of *TDRD3*$^{-/-}$ S2 cells was strongly reduced, whereas that of FMRP was largely unaffected (Figure 6C). The data are consistent with those in human and chicken, and indicate that in animals, Top3β but not FMRP requires TDRD3 to associate with polyribosomes.

DISCUSSION

RNA topoisomerase activity is present in Type IA topoisomerases from all domains of life

Here we show that RNA topoisomerase activity is present in Type IA topoisomerases from bacteria (EcoTop1 and TmaTop1), archaea (SsoTop3 and NeqTop3), and eukarya

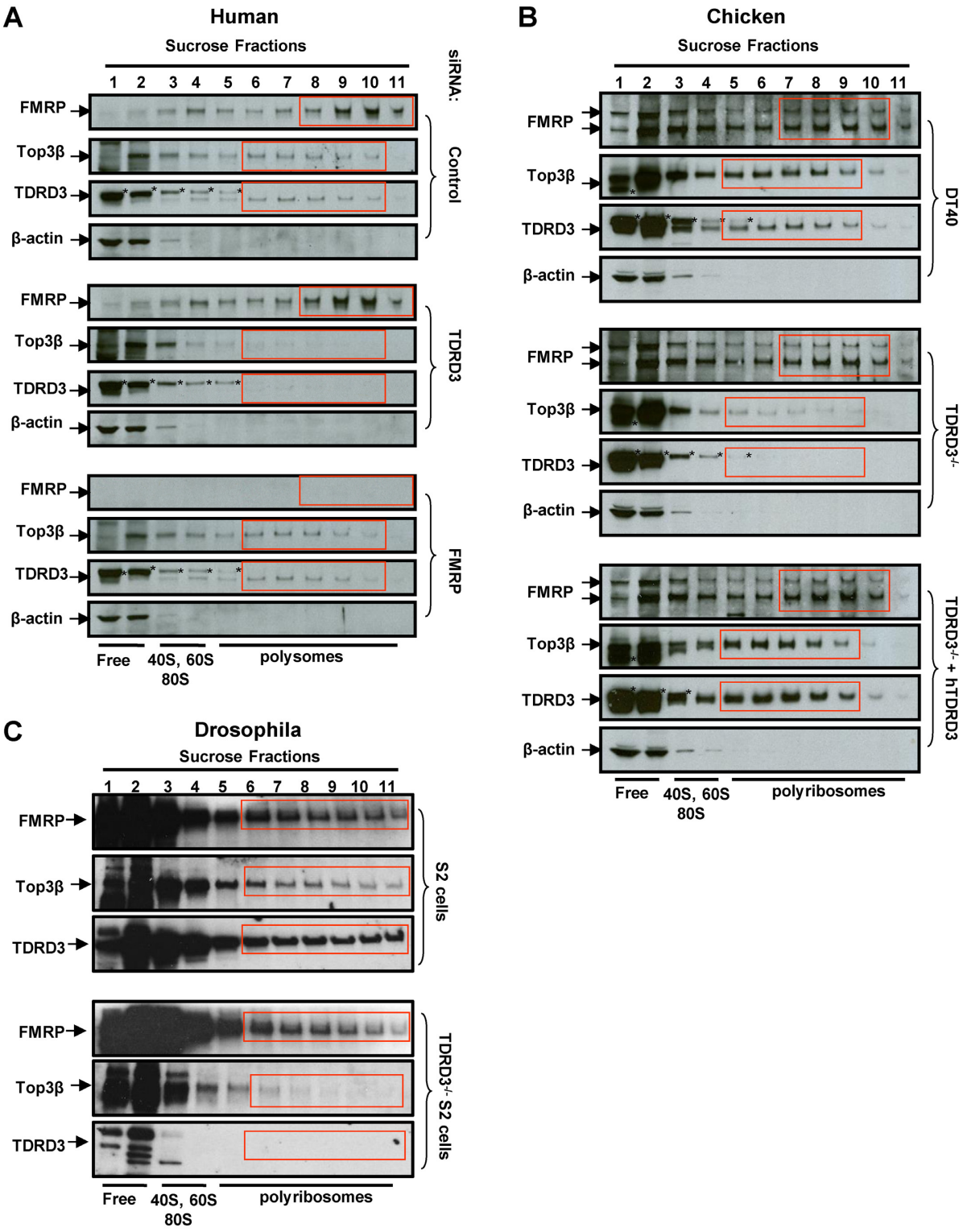

Figure 6. Top3β homologs from animals require TDRD3 for their association with polyribosomes. (**A**) Immunoblotting of sucrose gradient fractions of siRNA treated HEK293 cells shows that TDRD3 but not FMRP is required for polyribosome association of Top3β. Cytoplasmic extracts were prepared from the HEK293 cell transfected with a control siRNA oligo, or siRNA against TDRD3, or siRNA targeting FMRP, as indicated on the right. The Top panels of (**A**) were reproduced from our previous publication (4) for the convenience of readers. (**B**) Immunoblotting of sucrose gradient fractions of chicken DT40 cell lysate shows that TDRD3 is required for polyribosome association of Top3β but not FMRP. Cytoplasmic extracts were prepared from the wild-type, *TDRD3*$^{-/-}$ cells and *TDRD3*$^{-/-}$cells ectopically expressing human TDRD3 cDNA. (**C**) Immunoblotting of sucrose gradient fractions of wildtype and TDRD3-knockout Drosophila S2 cells shows that TDRD3 is essential for polyribosome association of Top3β but not FMRP. Cytoplasmic extracts were prepared from the wild-type and *TDRD3*$^{-/-}$ S2 cells. The red boxes highlight polyribosome fractions in which the indicated proteins display differences or no changes.

(yeast Top3 and human Top3β). Combined with earlier findings, these data demonstrate that RNA topoisomerase activity is prevalent in all three domains of life. Our data also show that Type IA topoisomerases have evolved from enzymes with dual activities in unicellular organisms (bacteria, archaea and yeast) into multi-protein complexes with restricted activities in animals (Figure 7A). For example, two Type IA enzymes from *E. coli* (Top1 and Top3) have dual activities for both DNA and RNA, whereas only one of the two human Type IA paralogs (Top3β) has RNA topoisomerase activity. Moreover, the two human Top3 paralogs comprise distinct complexes (4), with the Top3β complex containing a RBP (FMRP) and the Top3α complex a DNA helicase (BLM). The data suggest that Type IA topoisomerases have evolved into functionally distinct complexes in animals, with only Top3β complex acting on RNA. It should be mentioned that Top3β also has DNA topoisomerase activity (11), and can reduce transcription-induced R-loops (52). Thus, the Top3β complex may work in both DNA and RNA metabolism.

Type IA enzymes are among very few proteins that are involved in DNA metabolism and are also present in nearly all organisms (53). They have been proposed to exist in the Last Unknown Common Ancestors (LUCAs) for the three domains of life (53,54). It has been postulated that life started with a pool of self-replicating RNAs, and that an RNA world with RNA genome preceded the current DNA world (55). It has also been hypothesized that LUCAs may have an RNA genome, or an RNA/DNA hybrid genome, or a DNA genome with an RNA replication intermediate (53,56,57) (Figure 7B). The finding that Type IA enzymes possess RNA topoisomerase activity supports these RNA genome-based hypotheses. Moreover, the result implies that Type IA enzymes may have originated in the RNA world to solve RNA topological problems during duplication and segregation of the RNA genome (Figure 7B); these roles may be comparable to those of DNA topoisomerases, which are essential in replication and segregation of the DNA genome. When much of the RNA function was eventually replaced by DNA, many Type IA enzymes retained their RNA activity while developing additional activity for DNA. This could rationalize the prevalence of the RNA topoisomerase activity in Type IA enzymes.

RNA and DNA topoisomerases partially overlap in mechanism

Which domains are required for RNA topoisomerase activity, and is this requirement the same for the DNA topoisomerase activity? Our analyses of EcoTop1 mutants revealed that the conserved Type IA core domains are both necessary and sufficient for its RNA topoisomerase activity, whereas the non-conserved CTD is dispensable. This feature resembles that of EcoTop1 topoisomerase activity in DNA catenation assay, which also depends on the core domain but not on the CTD (34). Moreover, the strictly conserved catalytic Tyr residue essential for the DNA topoisomerase reaction is also necessary for RNA topoisomerase activity of all Type IA enzymes tested from bacteria, archaea, and eukaryotes. We infer that DNA and RNA topoisomerase reactions share common mechanisms, including the use of the same catalytic Tyr residue.

Although the CTD is dispensable for EcoTop1 in RNA topoisomerase reaction, it is required for the relaxation of supercoiled DNA and for rescuing the temperature-sensitivity phenotype of its mutant (32). These results suggest that the DNA relaxation activity may have evolved after the RNA topoisomerase activity. We hypothesize that in the RNA world, the ancestral RNA topoisomerase may have contained only the conserved Type IA core domain, which is sufficient for its RNA topoisomerase activity; and later in the DNA world, the enzyme acquired the CTD domain and developed DNA relaxation activity. The large diversity in CTDs observed in Type IA enzymes from different species is consistent with its late acquisition. The evolution of RNA topoisomerases is further exemplified by findings that although CTD is dispensable for RNA topoisomerase activity of EcoTop1, it is critical for the activity of humTop3β. Moreover, the CTD of humTop3β has a unique RGG RNA-binding motif absent in humTop3α, which is also important for the RNA topoisomerase activity (4).

Why does Top3β from animals require its CTD domain for RNA topoisomerase activity, whereas bacterial Top1 does not? One possible explanation is that the Type IA core domains in Top3 homologs of animals (Top3α and Top3β) may have evolved to possess low RNA-binding affinity, in contrast to those from bacterial and yeast that have high RNA affinity. The low RNA-affinity core domains allow animals to use a CTD of high RNA affinity and a CTD of low affinity to distinguish its RNA topoisomerase (Top3β) from its DNA topoisomerase (Top3α), respectively. The advantage of such a system is that it can prevent the DNA topoisomerase (Top3α) from being trapped mistakenly by RNA molecules and mislocalized in non-functional compartments, such as the cytoplasm. Consistent with this hypothesis, only Top3β, but not Top3α, localizes in cytoplasmic RNA stress granules (4) and stably associates with mRNAs in cells (58,59).

RNA topoisomerases from animals have TDRD3-dependent association with polyribosomes

We and others have recently discovered that human Top3β, together with its interacting partners TDRD3 and FMRP, associate with polyribosomes, the machine of mRNA translation (4,5). Here we extended this analysis and found that Top3β, TDRD3, and FMRP homologs from other animals (chicken and Drosophila) also associate with polyribosomes. In contrast, Top3β homologs from the yeast and bacteria have no detectable association. The data suggest that during evolution, RNA topoisomerases in animals have acquired unique features that allow them to function in mRNA translation as part of polyribosomes. Consistent with this suggestion, Top3β homologs in animals have at least two structural features that are absent in their counterparts in yeast, archaea and bacteria: one, they contain the unique RGG RNA binding motif; and two, they form a stable complex with TDRD3 and FMRP. We further demonstrated that the polyribosome association of Top3β homologs in human, chicken and Drosophila cells all require TDRD3 (but not FMRP). Because TDRD3 is capa-

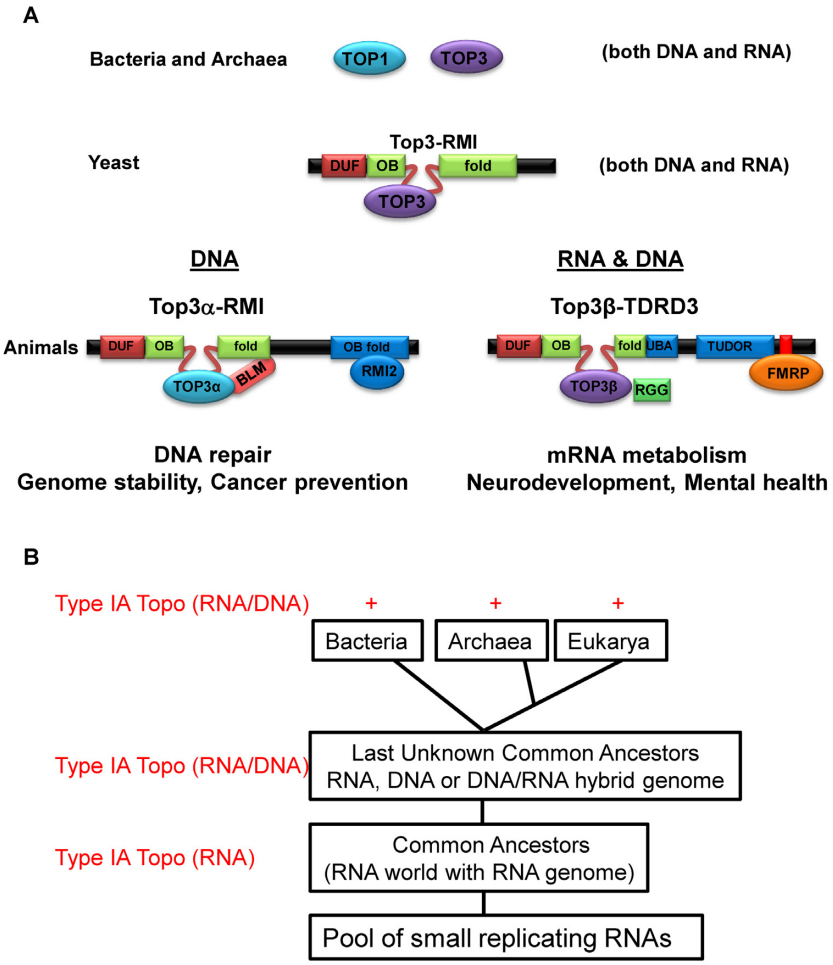

Figure 7. Type IA topoisomerases have evolved from enzymes with dual activities in microorganisms to multi-protein complexes with distinct functions in animals; RNA topoisomerases may originate in the RNA world and are conserved through evolution. (**A**) Schematic representation of evolution of Type IA topoisomerases in DNA and RNA metabolism. In *E. coli*, both Type IA enzymes (Top1 and Top3) have dual activities that can catalyze topoisomerase reactions on DNA and RNA. In yeast, the only Type IA enzyme is part of a complex (Top3-Rmi1) that also has dual activities for DNA and RNA. In human, only one of the two Type IA paralogs, Top3β, has RNA topoisomerase activity, whereas Top3α does not. Interestingly, Top3β, but not Top3α, has acquired during evolution a *bona fide* RNA-binding domain (RGG box) that is required for its RNA topoisomerase activity. Moreover, the two Top3 paralogs comprise two distinct complexes, with the Top3β complex containing a RNA binding protein (FMRP), whereas the Top3α complex containing a DNA helicase (BLM). These data argue that Type IA topoisomerases have evolved into two functional distinct complexes in animals, one for RNA and DNA (Top3β-TDRD3-FMRP), and one for DNA only (Top3α-Rmi1-Rmi2-BLM). (**B**) A model of origin and evolution of Type IA topoisomerases and their activity for RNA and DNA. It has been postulated that life starts with a pool of self-replicating RNAs; and there exists an RNA world with RNA genome prior to the current DNA world. We propose that Type IA enzymes may originate in the RNA world to solve topological problems during RNA metabolism. When the RNA world evolved and was eventually replaced by the DNA world, many of these enzymes retained their RNA topoisomerase activity while developing a new activity for DNA. This may explain the prevalence of the RNA topoisomerase activity in Type IA enzymes from all three domains.

ble of interacting with multiple translation factors through its different protein-binding modules, such as Tudor domain, FMRP-binding motif, and EBM motif (4,5,7,8), it may act as a bridge that targets Top3β to polyribosomes and other translation components. We propose that Top3β and TDRD3 work coordinately as a complex on polyribosomes to regulate mRNA translation in animals.

It should be pointed out that although Type IA enzymes can catalyze RNA topoisomerase reactions in vitro and associate with polyribosomes in vivo, it remains to be determined whether they actually catalyze RNA topoisomerase reactions in vivo. Future work is necessary to identify the exact RNA metabolic reactions that require these topoisomerases. In addition, the TDRD3 homologs from plants are structurally different from those of animals in their C-terminal domains: they lack the Tudor, UBA and FMRP-interaction domains, but contain a predicted RGG-RNA-binding motif (Supplemental Figure S7A) (4), hinting that they may interact with RNA differently compared to their animal counterparts. Whether plant Top3β associates with polyribosome in a TDRD3-dependent manner remains to be investigated.

The RNA topoisomerase complex Top3β-TDRD3 originates in unicellular eukaryotes and has evolved into two distinct forms in animals and plants

Our phylogenetic analyses of the current NCBI database revealed several interesting observations regarding evolution of Top3β–TDRD3 complex. First, while yeast has a single Top3 protein, several species of fungi have two distinctive Top3 paralogs, with one resembling Top3α and the other one Top3β (Supplemental Figure S7A), indicating that Top3β diverged from Top3α in unicellular eukaryotes. Second, we have previously noted that Top3β in animals and plants contains a distinctive RGG box at its C-terminus; and this box is absent in Top3α from animals (4). Here we find that the RGG box is conserved in not only Top3β, but also Top3α, in both fungi and plants (Supplemental Figure S7A and S7B); but it is absent in Type IA enzymes of yeast, bacteria and archaea. These findings imply that the eukaryotic ancestor of Type IA topoisomerases may have acquired the RGG box through gene-fusion prior to its duplication and subsequent divergence into two distinctive Top3 paralogs. In animals, Top3α may have lost its RGG box after the enzyme became an exclusive DNA topoisomerase, so that this RNA-binding box became dispensable. Third, TDRD3 co-exists with Top3β in not only animals and plants, but also several species of fungi (Supplemental Figures S7A, S8, and S9). In contrast, FMRP is present only in animals (Supplemental Figures S7A and S10). The data suggest that the Top3β–TDRD3 complex originated in unicellular eukaryotes and is conserved in both animals and plants, whereas the Top3β–TDRD3–FMRP complex was created later during evolution and existed in only animals. Fourth, TDRD3 homologs in fungi lack the C-terminal Tudor, UBA, and the FMRP-binding motif, which are present in TDRD3 of animals but absent in TDRD3 of plants (Supplemental Figure S7A). Notably, TDRD3 from several species of fungi also contain a predicted RGG box, which is present in TDRD3 of plants but not animals, suggesting that the Top3β–TDRD3 complex in animals may have diverged more from its ancestor than the one in fungi and plants. It would be interesting to study whether both Top3α and Top3β complexes from fungi and plants have RNA topoisomerase activity, which may reveal unique mechanisms of these enzymes in RNA metabolism.

SUPPLEMENTARY DATA

Supplementary Data are available at NAR Online.

ACKNOWLEDGEMENTS

We thank S. Brill for providing V5-tagged yeast top3 strains, K. Marians for *E. coli* Top3 reagents, A. Emili for SPA-tagged *E. coli* Top1 and Top3 strains. We thank Dr D. Schlessinger for critical reading of the manuscript.
Author contributions: M.A., W.S., W.L., Y.X., J.M., H.D., F.L., H.Z., Q.W., G.E.S., H.N. and D.X. conducted experiments; S.Z., T.S.H., Y.T.D., M.G., D.X. and W.W. supervised the projects; M.A., W.S., Y.X., S.Z., M.C., M.N., F.L., H.N., Y.P., T.S.H., Y.T.D., D.X. and W.W. provided reagents and analyzed the data; M.A., W.S., D.X. and W.W. wrote the manuscript with input from the other authors.

FUNDING

Intramural Research Program of the National Institute on Aging [Z01 AG000657-08]; National Cancer Institute [Z01 BC006161]; National Institutes of Health; the National Basic Research Program of China [2013CB911002)]; National Natural Science Foundation of China [31271435]. Funding for open access charge: National Institute on Aging, NIH, Intramural funding.
Conflict of interest statement. None declared.

REFERENCES

1. Wang,J.C. (1971) Interaction between DNA and an Escherichia coli protein omega. *J. Mol. Biol.*, **55**, 523–533.
2. Wang,J.C. (2002) Cellular roles of DNA topoisomerases: a molecular perspective. *Nat. Rev. Mol. Cell Biol.*, **3**, 430–440.
3. Wang,H., Di Gate,R.J. and Seeman,N.C. (1996) An RNA topoisomerase. *Proc. Natl. Acad. Sci. U.S.A.*, **93**, 9477–9482.
4. Xu,D., Shen,W., Guo,R., Xue,Y., Peng,W., Sima,J., Yang,J., Sharov,A., Srikantan,S., Fox,D. 3rd *et al.* (2013) Top3beta is an RNA topoisomerase that works with fragile X syndrome protein to promote synapse formation. *Nat. Neurosci.*, **16**, 1238–1247.
5. Stoll,G., Pietilainen,O.P., Linder,B., Suvisaari,J., Brosi,C., Hennah,W., Leppa,V., Torniainen,M., Ripatti,S., Ala-Mello,S. *et al.* (2013) Deletion of TOP3beta, a component of FMRP-containing mRNPs, contributes to neurodevelopmental disorders. *Nat. Neurosci.*, **16**, 1228–1237.
6. Darnell,J.C., Van Driesche,S.J., Zhang,C., Hung,K.Y., Mele,A., Fraser,C.E., Stone,E.F., Chen,C., Fak,J.J., Chi,S.W. *et al.* (2011) FMRP stalls ribosomal translocation on mRNAs linked to synaptic function and autism. *Cell*, **146**, 247–261.
7. Linder,B., Plottner,O., Kroiss,M., Hartmann,E., Laggerbauer,B., Meister,G., Keidel,E. and Fischer,U. (2008) Tdrd3 is a novel stress granule-associated protein interacting with the Fragile-X syndrome protein FMRP. *Hum. Mol. Genet.*, **17**, 3236–3246.
8. Goulet,I., Boisvenue,S., Mokas,S., Mazroui,R. and Cote,J. (2008) TDRD3, a novel Tudor domain-containing protein, localizes to cytoplasmic stress granules. *Hum. Mol. Genet.*, **17**, 3055–3074.
9. Mullen,J.R., Nallaseth,F.S., Lan,Y.Q., Slagle,C.E. and Brill,S.J. (2005) Yeast Rmi1/Nce4 controls genome stability as a subunit of the Sgs1-Top3 complex. *Mol. Cell. Biol.*, **25**, 4476–4487.
10. Butland,G., Peregrin-Alvarez,J.M., Li,J., Yang,W., Yang,X., Canadien,V., Starostine,A., Richards,D., Beattie,B., Krogan,N. *et al.* (2005) Interaction network containing conserved and essential protein complexes in *Escherichia coli*. *Nature*, **433**, 531–537.
11. Wilson,T.M., Chen,A.D. and Hsieh,T. (2000) Cloning and characterization of *Drosophila* topoisomerase IIIbeta. Relaxation of hypernegatively supercoiled DNA. *J. Biol. Chem.*, **275**, 1533–1540.
12. Sutherland,J.H. and Tse-Dinh,Y.C. (2010) Analysis of RuvABC and RecG involvement in the escherichia coli response to the covalent topoisomerase-DNA complex. *J. Bacteriol.*, **192**, 4445–4451.
13. Nurse,P., Levine,C., Hassing,H. and Marians,K.J. (2003) Topoisomerase III can serve as the cellular decatenase in *Escherichia coli*. *J. Biol. Chem.*, **278**, 8653–8660.
14. Iiizumi,S., Nomura,Y., So,S., Uegaki,K., Aoki,K., Shibahara,K., Adachi,N. and Koyama,H. (2006) Simple one-week method to construct gene-targeting vectors: application to production of human knockout cell lines. *BioTechniques*, **41**, 311–316.
15. Bassett,A.R., Tibbit,C., Ponting,C.P. and Liu,J.L. (2014) Mutagenesis and homologous recombination in Drosophila cell lines using CRISPR/Cas9. *Biol. Open*, **3**, 42–49.
16. Gratz,S.J., Wildonger,J., Harrison,M.M. and O'Connor-Giles,K.M. (2013) CRISPR/Cas9-mediated genome engineering and the promise of designer flies on demand. *Fly*, **7**, 249–255.
17. Narula,G., Annamalai,T., Aedo,S., Cheng,B., Sorokin,E., Wong,A. and Tse-Dinh,Y.C. (2011) The strictly conserved Arg-321 residue in the active site of *Escherichia coli* topoisomerase I plays a critical role in DNA rejoining. *J. Biol. Chem.*, **286**, 18673–18680.

18. Annamalai,T., Dani,N., Cheng,B. and Tse-Dinh,Y.C. (2009) Analysis of DNA relaxation and cleavage activities of recombinant *Mycobacterium tuberculosis* DNA topoisomerase I from a new expression and purification protocol. *BMC Biochem.*, **11**, 10–18.
19. Lee,S.H., Siaw,G.E., Willcox,S., Griffith,J.D. and Hsieh,T.S. (2013) Synthesis and dissolution of hemicatenanes by type IA DNA topoisomerases. *Proc. Natl. Acad. Sci. U.S.A.*, **110**, E3587–E3594.
20. Hsieh,T.S. and Capp,C. (2005) Nucleotide- and stoichiometry-dependent DNA supercoiling by reverse gyrase. *J. Biol. Chem.*, **280**, 20467–20475.
21. Valenti,A., De Felice,M., Perugino,G., Bizard,A., Nadal,M., Rossi,M. and Ciaramella,M. (2012) Synergic and opposing activities of thermophilic RecQ-like helicase and topoisomerase 3 proteins in Holliday junction processing and replication fork stabilization. *J. Biol. Chem.*, **287**, 30282–30295.
22. Niu,H., Chung,W.H., Zhu,Z., Kwon,Y., Zhao,W., Chi,P., Prakash,R., Seong,C., Liu,D., Lu,L. *et al.* (2010) Mechanism of the ATP-dependent DNA end-resection machinery from *Saccharomyces cerevisiae*. *Nature*, **467**, 108–111.
23. Jamroze,A., Perugino,G., Valenti,A., Rashid,N., Rossi,M., Akhtar,M. and Ciaramella,M. (2014) The reverse gyrase from *Pyrobaculum calidifontis*, a novel extremely thermophilic DNA topoisomerase endowed with DNA unwinding and annealing activities. *J. Biol. Chem.*, **289**, 3231–3243.
24. Valenti,A., Perugino,G., D'Amaro,A., Cacace,A., Napoli,A., Rossi,M. and Ciaramella,M. (2008) Dissection of reverse gyrase activities: insight into the evolution of a thermostable molecular machine. *Nucleic Acids Res.*, **36**, 4587–4597.
25. Capp,C., Qian,Y., Sage,H., Huber,H. and Hsieh,T.S. (2010) Separate and combined biochemical activities of the subunits of a naturally split reverse gyrase. *J. Biol. Chem.*, **285**, 39637–39645.
26. Rodriguez,A.C. and Stock,D. (2002) Crystal structure of reverse gyrase: insights into the positive supercoiling of DNA. *EMBO J.*, **21**, 418–426.
27. Seol,Y., Zhang,H., Pommier,Y. and Neuman,K.C. (2012) A kinetic clutch governs religation by type IB topoisomerases and determines camptothecin sensitivity. *Proc. Natl. Acad. Sci. U.S.A.*, **109**, 16125–16130.
28. Qin,D. and Fredrick,K. (2013) Analysis of polysomes from bacteria. *Methods Enzymol.*, **530**, 159–172.
29. Pospisek,M. and Valasek,L. (2013) Polysome profile analysis–yeast. *Methods Enzymol.*, **530**, 173–181.
30. Al-Jubran,K., Wen,J., Abdullahi,A., Roy Chaudhury,S., Li,M., Ramanathan,P., Matina,A., De,S., Piechocki,K., Rugjee,K.N. *et al.* (2013) Visualization of the joining of ribosomal subunits reveals the presence of 80S ribosomes in the nucleus. *RNA*, **19**, 1669–1683.
31. Changela,A., DiGate,R.J. and Mondragon,A. (2001) Crystal structure of a complex of a type IA DNA topoisomerase with a single-stranded DNA molecule. *Nature*, **411**, 1077–1081.
32. Zumstein,L. and Wang,J.C. (1986) Probing the structural domains and function *in vivo* of *Escherichia coli* DNA topoisomerase I by mutagenesis. *J. Mol. Biol.*, **191**, 333–340.
33. Narula,G. and Tse-Dinh,Y.C. (2012) Residues of *E. coli* topoisomerase I conserved for interaction with a specific cytosine base to facilitate DNA cleavage. *Nucleic Acids Res.*, **40**, 9233–9243.
34. Ahumada,A. and Tse-Dinh,Y.C. (2002) The role of the Zn(II) binding domain in the mechanism of E. coli DNA topoisomerase I. *BMC Biochem.*, **3**, 13.
35. Tan,K., Zhou,Q., Cheng,B., Zhang,Z., Joachimiak,A. and Tse-Dinh,Y.C. (2015) Structural basis for suppression of hypernegative DNA supercoiling by *E. coli* topoisomerase I. *Nucleic Acids Res.*, **43**, 11031–11046.
36. Lima,C.D., Wang,J.C. and Mondragon,A. (1993) Crystallization of a 67 kDa fragment of Escherichia coli DNA topoisomerase I. *J. Mol. Biol.*, **232**, 1213–1216.
37. Cheng,B., Annamalai,T., Sorokin,E., Abrenica,M., Aedo,S. and Tse-Dinh,Y.C. (2009) Asp-to-Asn substitution at the first position of the DxD TOPRIM motif of recombinant bacterial topoisomerase I is extremely lethal to E. coli. *J. Mol. Biol.*, **385**, 558–567.
38. Viard,T., Lamour,V., Duguet,M. and Bouthier de la Tour,C. (2001) Hyperthermophilic topoisomerase I from *Thermotoga maritima*. A very efficient enzyme that functions independently of zinc binding. *J. Biol. Chem.*, **276**, 46495–46503.
39. Narula,G., Becker,J., Cheng,B., Dani,N., Abrenica,M.V. and Tse-Dinh,Y.C. (2010) The DNA relaxation activity and covalent complex accumulation of *Mycobacterium tuberculosis* topoisomerase I can be assayed in *Escherichia coli*: application for identification of potential FRET-dye labeling sites. *BMC Biochem.*, **11**, 41.
40. Dai,P., Wang,Y., Ye,R., Chen,L. and Huang,L. (2003) DNA topoisomerase III from the hyperthermophilic archaeon *Sulfolobus solfataricus* with specific DNA cleavage activity. *J. Bacteriol.*, **185**, 5500–5507.
41. Chen,C.F. and Brill,S.J. (2007) Binding and activation of DNA topoisomerase III by the Rmi1 subunit. *J. Biol. Chem.*, **282**, 28971–28979.
42. Chang,M., Bellaoui,M., Zhang,C., Desai,R., Morozov,P., Delgado-Cruzata,L., Rothstein,R., Freyer,G.A., Boone,C. and Brown,G.W. (2005) RMI1/NCE4, a suppressor of genome instability, encodes a member of the RecQ helicase/Topo III complex. *EMBO J.*, **24**, 2024–2033.
43. Stewart,L., Redinbo,M.R., Qiu,X., Hol,W.G. and Champoux,J.J. (1998) A model for the mechanism of human topoisomerase I. *Science*, **279**, 1534–1541.
44. McCoubrey,W.K. Jr and Champoux,J.J. (1986) The role of single-strand breaks in the catenation reaction catalyzed by the rat type I topoisomerase. *J. Biol. Chem.*, **261**, 5130–5137.
45. Kim,N., Huang,S.N., Williams,J.S., Li,Y.C., Clark,A.B., Cho,J.E., Kunkel,T.A., Pommier,Y. and Jinks-Robertson,S. (2011) Mutagenic processing of ribonucleotides in DNA by yeast topoisomerase I. *Science*, **332**, 1561–1564.
46. Sekiguchi,J. and Shuman,S. (1997) Site-specific ribonuclease activity of eukaryotic DNA topoisomerase I. *Mol. Cell*, **1**, 89–97.
47. Carey,J.F., Schultz,S.J., Sisson,L., Fazzio,T.G. and Champoux,J.J. (2003) DNA relaxation by human topoisomerase I occurs in the closed clamp conformation of the protein. *Proc. Natl. Acad. Sci. U.S.A.* **100**, 5640–5645.
48. Zhang,H., Meng,L.H. and Pommier,Y. (2007) Mitochondrial topoisomerases and alternative splicing of the human TOP1mt gene. *Biochimie*, **89**, 474–481.
49. Anderson,B.G. and Stivers,J.T. (2014) Variola type IB DNA topoisomerase: DNA binding and supercoil unwinding using engineered DNA minicircles. *Biochemistry*, **53**, 4302–4315.
50. Wang,Y., Knudsen,B.R., Bjergbaek,L., Westergaard,O. and Andersen,A.H. (1999) Stimulated activity of human topoisomerases IIalpha and IIbeta on RNA-containing substrates. *J. Biol. Chem.*, **274**, 22839–22846.
51. Yin,J., Sobeck,A., Xu,C., Meetei,A.R., Hoatlin,M., Li,L. and Wang,W. (2005) BLAP75, an essential component of Bloom's syndrome protein complexes that maintain genome integrity. *EMBO J.*, **24**, 1465–1476.
52. Yang,Y., McBride,K.M., Hensley,S., Lu,Y., Chedin,F. and Bedford,M.T. (2014) Arginine methylation facilitates the recruitment of TOP3B to chromatin to prevent R loop accumulation. *Mol. Cell*, **53**, 484–497.
53. Leipe,D.D., Aravind,L. and Koonin,E.V. (1999) Did DNA replication evolve twice independently? *Nucleic Acids Res.*, **27**, 3389–3401.
54. Forterre,P. and Gadelle,D. (2009) Phylogenomics of DNA topoisomerases: their origin and putative roles in the emergence of modern organisms. *Nucleic Acids Res.*, **37**, 679–692.
55. Poole,A.M. and Logan,D.T. (2005) Modern mRNA proofreading and repair: clues that the last universal common ancestor possessed an RNA genome? *Mol. Biol. Evol.*, **22**, 1444–1455.
56. Forterre,P. (2006) Three RNA cells for ribosomal lineages and three DNA viruses to replicate their genomes: a hypothesis for the origin of cellular domain. *Proc. Natl. Acad. Sci. U.S.A.*, **103**, 3669–3674.
57. Forterre,P., Gribaldo,S., Gadelle,D. and Serre,M.C. (2007) Origin and evolution of DNA topoisomerases. *Biochimie*, **89**, 427–446.
58. Baltz,A.G., Munschauer,M., Schwanhausser,B., Vasile,A., Murakawa,Y., Schueler,M., Youngs,N., Penfold-Brown,D., Drew,K., Milek,M. *et al.* (2012) The mRNA-bound proteome and its global occupancy profile on protein-coding transcripts. *Mol. Cell*, **46**, 674–690.
59. Castello,A., Fischer,B., Eichelbaum,K., Horos,R., Beckmann,B.M., Strein,C., Davey,N.E., Humphreys,D.T., Preiss,T., Steinmetz,L.M. *et al.* (2012) Insights into RNA biology from an atlas of mammalian mRNA-binding proteins. *Cell*, **149**, 1393–1406.